Available online at www.sciencedirect.com
ScienceDirect
Ceramics International 35 (2009) 1953–1959
CERAMICS INTERNATIONAL
www.elsevier.com/locate/ceramint

Foaming of flat glass cullet using Si_3N_4 and MnO_2 powders

Alejandro Saburit Llaudis [a], María José Orts Tari [a], Francisco Javier García Ten [a], Enrico Bernardo [b,*], Paolo Colombo [c]

[a] *Instituto de Tecnología Cerámica (ITC), Asociación de Investigación de las Industrias Cerámicas (AICE), Universitat Jaume I, Campus Universitario Riu Sec, Avda. Vicent Sos Baynat, 12006 Castellón, Spain*
[b] *Dipartimento di Ingegneria Meccanica – Settore Materiali, Università di Padova, via Marzolo, 9, 35131 Padova, Italy*
[c] *Department of Materials Science and Engineering, The Pennsylvania State University, University Park, PA 16802, USA*

Received 6 October 2008; received in revised form 12 October 2008; accepted 22 October 2008
Available online 17 November 2008

Abstract

The introduction of a compound capable of releasing oxygen, such as MnO_2, greatly improves the foaming ability of Si_3N_4 used as foaming agent in soda-lime glass powder, leading to expansion at a relatively low temperature (800–850 °C) and short processing time (7–30 min). The effect is based on the supply of oxygen, in addition to that in the furnace atmosphere. At the highest level of porosity, however, the strength of foams is negatively affected by a coarse microstructure, determined by cell coalescence. The reduction of firing temperature or, above all, the reduction of the processing time, was found to limit the coalescence and significantly improve the strength of the foams.

Keywords: B. Porosity; D. Glass; Foam

1. Introduction

Glass foams are attracting a growing interest for thermal and acoustic insulation applications [1]. Compared to the polymeric foams currently employed, they possess significant advantages. Firstly, they exhibit a superior chemical and thermal stability, important for durability and safety reasons (the combustion of polymeric foams generally leads to the evolution of potentially toxic gases, while glass foams, due to their inorganic nature, are un-inflammable) [2]. Secondly, glass foams generally possess a significant mechanical strength, which is useful in structural applications; as an example, there is an increasing demand for glass foams in the form of pellets or loose pieces, to be used as aggregates for lightweight concrete [3]. The production of glass foams may follow two distinct processes. The first, dating back to the 1930s, consists of the direct introduction of gases (''blowing'') into molten glass [4]. The second, much less expensive, is based on the viscous flow sintering of fine glass powders, which creates a pyroplastic mass which is foamed by the action of specific powder additives (foaming agents) [5–7]. Besides significant energy savings (the sintering of glass occurs at a much lower temperature than that required by blowing), the second process brings fundamental environmental advantages, since the glass powder mixture may contain many different types of crushed recycled glass, including glasses deriving from the vitrification of inorganic waste [8–16].

The present investigation focuses on the production of foam glass from flat glass cullet. Although recommended for limiting the consumption of energy and natural raw materials, the usage of cullet in the manufacturing of new glass articles is not simple. In fact, only glass cullet with well-controlled composition is generally accepted in conventional (flat glass, glass containers) products. Glass foams, for which the purity is not essential, therefore represent a promising way of fabricating ''fully recycled'' glass-based components. The foaming mechanism is an essential point to be considered [1]. It may be based on decomposition or oxidation reactions. The decomposition reactions derive from the presence of carbonates and sulphates, while oxidation reactions are determined by the interaction of carbon-containing species (C, SiC) with oxygen, coming mainly from the atmosphere of the sintering furnace. In both cases, the foaming corresponds to the release of CO, CO_2 or SO_3 gases, which may represent an environmental problem (toxicity, greenhouse effect, etc.). Although quite more expensive than

* Corresponding author. Tel.: +39 049 8275510; fax: +39 049 8275505.
E-mail address: enrico.bernardo@unipd.it (E. Bernardo).

0272-8842/$34.00
doi:10.1016/j.ceramint.2008.10.022

any other foaming agent, silicon nitride (Si_3N_4) is interesting, since it provides an oxidation/decomposition reaction ($Si_3N_4 + 3O_2 \rightarrow 3SiO_2 + 2N_2$), with simply nitrogen as the foaming gas. In the present investigation we present an optimization of the foaming reaction, focused on the introduction of oxygen not only from the sintering atmosphere, but also from an oxidizing agent, i.e. an oxide of a metal with multiple valence state, such as MnO_2. This oxide has been already used as a foaming agent by simple decomposition [17]. The present work is aimed at exploiting the peculiarities of the Si_3N_4/oxidizing agent coupling.

2. Experimental procedure

Recycled float glass was used as starting material (true density $\rho = 2.52$ g/cm^3). The glass fragments were ground in a hammer mill until reaching a particle size below 500 μm ($d_{50} = \sim 200$ μm). Si_3N_4 powder (H.C. Starck Ceramics, Selb, Germany) was used as foaming agent (3 wt%), and MnO_2 powder (reagent grade, Mallinckrodt Chemical Inc., St. Louis, MO, USA) was added to promote the oxidation of Si_3N_4 at elevated temperatures, in different amounts. The average particle size of Si_3N_4 and MnO_2 was 0.56 and 5.95 μm, respectively, and their true density 3.19 and 5.03 g/cm^3. Batches were obtained by dry mixing the components in a planetary mill for 10 min. Polyethylene glycol (PEG-400; 5 wt%) was added to improve the pressing of the glass powders. Uniaxial pressing was conducted at 30 MPa in a laboratory press, and cylindrical pellets of 35 mm in diameter and 6 mm thick were obtained. The samples were dried in an oven at 110 °C and their bulk density was measured by dividing the weight of the sample by its volume. The specimens were then fired in air, in an electric laboratory furnace with a heating rate of 40 °C/min, at different maximum temperatures (in the range 800–900 °C) and with different soaking times (7–30 min), to evaluate the effect of these parameters on the characteristics of the glass foams. Natural convection inside the furnace was used for cooling. True density was measured using an helium pycnometer (Micromeritics AccuPyc 1330, Norcross, GA) and the apparent density, and amount of open and closed porosity was evaluated by the Archimedes method. Water absorption was measured as the weight gain after placing the samples 2 h in boiling water. Compressive strength was measured using an UTM machine (Instron 1121, Norwood, MA, USA) with a crosshead speed of 1 mm/min on prismatic samples with an average size of 8 mm × 8 mm × 3 mm, cut from the disks. At least 5 tests were conducted for each specimen. The morphology of the foams was studied with a scanning electron microscope (SEM, Philips XL 30, Eindhoven, The Netherlands) and the crystalline phases present in the foamed pieces were assessed using X-ray diffraction (XRD, Philips PW 3710, Eindoven, The Netherlands). Image Analysis (Image Tool 3.0, UTHSCSA, USA) was used to quantify the average cell size and cell size distribution. Simultaneous Thermal analysis (DTA/TGA, Netzsch STA409, Selb, Germany; heating rate 10 °C/min) was performed in static air on selected samples. Dilatometry (Netzsch DIL402, Selb, Germany; heating rate 10 °C/min) was used to determine the glass transition (T_g) and the softening temperature (T_R) of the glass.

3. Results and discussion

3.1. Influence of MnO_2 content

When Si_3N_4 is mixed with glass particles and pressed into a pellet (at temperatures below the glass transition temperature, T_g) the oxygen necessary for carrying out the reaction diffuses via the porosity available. The amount of oxygen available inside the glass pellet, upon softening (at temperatures above T_g) may not be sufficient to complete the oxidation reaction. Therefore, the introduction of substances that generate oxygen at elevated temperatures, such as MnO_2, may improve the oxidation of Si_3N_4. Mn is a metal with multiple valence state (Mn^{4+}, Mn^{3+}, Mn^{2+}) [18]. The oxide with the highest valence state, MnO_2 (pyrolusite), decomposes into oxides with a lower valence state (Mn_2O_3, Mn_3O_4, MnO) and oxygen. MnO (manganosite) has been effectively found, in reducing conditions (as an example, in carbon monoxide), from the decomposition of higher manganese oxides [19]. If we consider the oxides with the highest and the lowest oxidation states, we have the largest release of oxygen, as follows: $2MnO_2 \rightarrow 2MnO + O_2$.

The oxidizing ability (i.e. thermal decomposition with oxygen release) has been exploited for many centuries for decolorizing glass (the reduction of manganese ions promotes the oxidation of low valence state ions, such as Fe^{2+} and Cr^{2+}, which have a high molar extinction coefficient, into high valence ions possessing a lower molar extinction coefficient, and therefore develop a less intense color in the glass) [20].

In the hypothesis of an oxidation of Si_3N_4 provided only by the complete reduction of MnO_2 into MnO (to be dissolved in the glass), we obtain: $Si_3N_4 + 6MnO_2 \rightarrow 3SiO_2 + 6MnO + 2N_2$. MnO_2 was added in amounts varying from zero to the quantity necessary to complete the hypothetic reaction of $Si_3N_4 + MnO_2$ reported above (i.e. the MnO_2/Si_3N_4 molar ratio varied from 0 to 6). The firing temperature range was selected between 800 and 900 °C, bearing in mind the requirement of reducing the cost of the process by maintaining a low maximum firing temperature, suitable for the selected raw materials. The softening temperature (T_R) value of 630 °C, from dilatometric analysis, is consistent with a significant viscous flow at the selected temperatures (viscous flow sintering occurs at a temperature at least 50 °C higher than T_R [21,22]). DTA/TGA analysis performed on Si_3N_4 and MnO_2 powders (not reported here for the sake of brevity) showed that the oxidation of silicon nitride occurs in a significant way at temperatures >1100 °C, while MnO_2 presents two weight losses, attributable to the oxygen release associated to the transformation into oxides with a lower valence state of Mn ions, at about 610 °C (from MnO_2 to Mn_2O_3, with a weight loss of about 9%) and 920 °C (from Mn_2O_3 to Mn_3O_4, with a weight loss of about 3%). The pyrolusite/silicon nitride mixture in stoichiometric amount ($MnO_2/Si_3N_4 = 6$) exhibits a significant weight loss at 900–1000 °C, with a weight loss of about 9%, which is effectively consistent with the MnO_2/MnO reduction and release of nitrogen.

Table 1
Physical properties of foams obtained using different MnO_2 amounts (Si_3N_4 = 3.5 wt%, 15 min at 850 °C). ρ_D = dry bulk density; ρ_F = fired bulk density; α = degree of foaming; σ = compressive strength; WA = water absorption.

Sample label	MnO_2/Si_3N_4 molar ratio (wt%)	ρ_D (kg/cm^3)	ρ_F (g/cm^3)	α	σ (MPa)	WA (%)
Glass	–	1.77 ± 0.01	2.43 ± 0.03	0.00	–	<0.1
A	6 (13.0%)	1.90 ± 0.01	0.20 ± 0.02	0.90	0.5 ± 0.1	23.2
B	3 (6.5%)	1.85 ± 0.01	0.31 ± 0.03	0.83	1.8 ± 0.4	22.9
C	1.5 (3.3%)	1.82 ± 0.01	0.51 ± 0.02	0.72	5.7 ± 0.8	4.0
D	0.75 (1.6%)	1.76 ± 0.01	0.86 ± 0.02	0.51	28 ± 5	1.3
E	0 (0.0%)	1.67 ± 0.01	1.35 ± 0.02	0.19	44 ± 8	<0.1

Table 1 reports the values of some physical properties of specimens treated at 850 °C for 15 min: dry (as pressed sample, after drying) and fired bulk density (ρ_D and ρ_F, respectively), water absorption (WA) and compressive strength (σ). Parameter α is included in the table to evaluate the degree of foaming reached for each composition. This parameter was calculated from the following equation:

$$\alpha = \frac{\rho_G - \rho_F}{\rho_G} \quad (1)$$

where ρ_G is the fired bulk density of glass specimens without foaming agents. The table shows that the values of ρ_D for the different compositions decrease as the percentage of MnO_2 is reduced. The data also indicate that the content of MnO_2 has a dramatic effect on the degree of expansion achieved in the fired components. The effect is particularly significant, since it is achieved at a relatively low temperature (850 °C; note that foams developed from soda-lime glass are usually fired at 900–950 °C [1,14]). The low firing temperature is important for avoiding any devitrification of the glass, which would hamper foaming of the mixture, as confirmed by the fact that all the samples where X-ray amorphous.

Fig. 1 reports the evolution of the bulk density and mechanical strength of samples fired at 850 °C, for 15 min, as a function of MnO_2 content, for compositions with 3.5 wt% of Si_3N_4. Composition E, without MnO_2, gives a bulk density value which is for relatively high for a foam and a low degree of expansion (α = 0.39), indicating that the foaming process was not very effective. This is probably due to the difficulty in oxidizing completely the Si_3N_4 powders. With the increase of the content of MnO_2, a strong decrease in the bulk density is observed. The decrease in bulk density in these compositions is reasonably due to the promotion of the oxidation of Si_3N_4, provided by MnO_2, with consequent generation of N_2. If the foaming would be attributed only to the decomposition of MnO_2, the decrease of density should be almost linear (at the same Si_3N_4 content). The observed trend, on the contrary, suggests a sort of saturation, i.e. a condition of minimum density, represented by the MnO_2/Si_3N_4 molar ratio equal to 6. It may also be noted that the density is substantially low even with a MnO_2/Si_3N_4 molar ratio equal to 3; this is consistent with the assumption, reported above, that MnO_2 is not the only source for oxygen (some oxygen may come from the air trapped between glass powders upon processing).

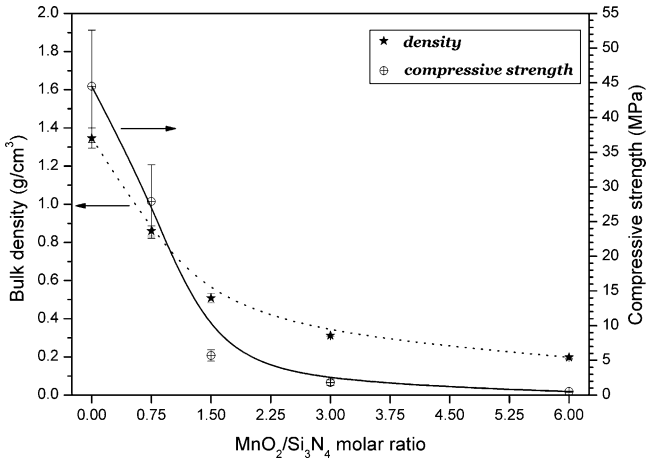

Fig. 1. Evolution of bulk density and compressive strength with MnO_2 amount (Si_3N_4 = 3.5 wt%, 15 min at 850 °C).

The microstructure of the fired samples can be observed in Fig. 2, and the cell size distribution is reported in Fig. 3. It can be observed that, with increasing the content of MnO_2, the porous structure changes significantly with respect to cell size, cell shape and strut/cell wall thickness, as well as in terms of total porosity. Thus, for low MnO_2 content (composition D) the porous morphology is formed by numerous cells of spherical shape, with size ranging from about 50 to 200 μm. These cells are mostly non-interconnected (WA values are very low) and have a mono-modal cell window size distribution. The increase of the MnO_2 content (composition C) produces an increase in the amount of porosity and in the cell size, as a result of the increased amount of gas generated within the sample. The cells maintain a fairly spherical shape and are still mostly non-interconnected; however, it is possible to observe an incipient coalescence among the cells (see arrows in Fig. 2c) and the WA value is higher. Coalescence leads to a decrease in the thickness of the cell walls as a result of coarsening of gas bubbles in the softened glass. With increasing cell dimension, there is a wider distribution of the average size (ranging from about 30 to 600 μm), and the cell size begins to show a bimodal distribution, with two peaks around 50 and 1000 μm. The smaller pores (~50 μm) are situated at the cell walls which enclose the larger pores.

Fig. 1 illustrates that the trend of the compressive strength, with increasing MnO_2 content, is similar to that observed for the bulk density. It is well known that both the amount of porosity and the morphology of porous structure define the mechanical strength of glass and ceramic foams [1,23,24]. The practical stabilization of compressive strength with high

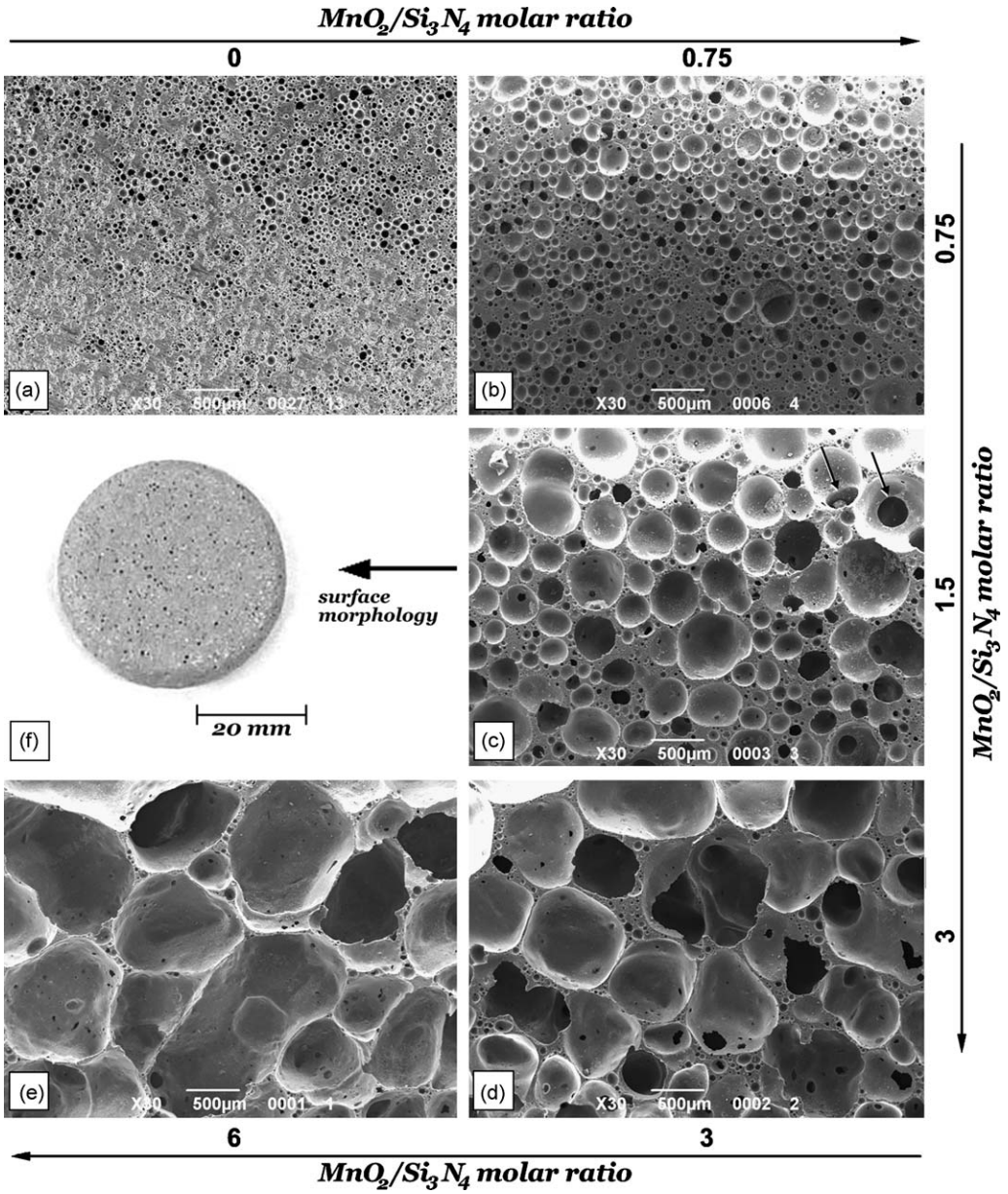

Fig. 2. Morphological evolution of glass foams with MnO_2 amount (Si_3N_4 = 3.5 wt%, 15 min at 850 °C): (a) MnO_2/Si_3N_4 = 0; (b) MnO_2/Si_3N_4 = 0.75; (c) MnO_2/Si_3N_4 = 1.5; (d) MnO_2/Si_3N_4 = 3; (e) MnO_2/Si_3N_4 = 6; (f) surface morphology of the sample with MnO_2/Si_3N_4 = 1.5.

MnO_2 contents may be associated to several contrasting effects. At a high level of porosity, it can be noted a reduction in the thickness of cell walls (struts), which is undoubtedly profitable for the mechanical strength (the failure of foams is classically associated to the bending of cell walls and edges; thin cell walls and edges are stronger, due to the reduced probability of finding critical flaws). This is effect is counterbalanced by the increase of the average cell size (macrocellular foams are generally weaker than microcellular ones, due to a less homogeneous stress distribution [25] and, above all, by the bimodal distribution. The presence of small pores in the cell walls, in fact, as previously observed [11,14], make closed cell foams, like glass foams, more similar to weaker open cell foams.

3.2. Influence of firing conditions

The firing conditions used to obtain the foams influences the viscosity of the softened glass, the extent at which the reduction/oxidation reactions occur and therefore the morphology of the samples and their properties. Fig. 4 illustrates the evolution of bulk density and compressive strength with firing temperature, starting from a selected (and constant) MnO_2 content (MnO_2/Si_3N_4 = 1.5). It may be noted that both variables decrease with increasing the firing temperature, although their trend is different in the temperature range studied (800–900 °C). Thus, while the evolution of bulk density is more limited and follows a linear trend, the variation in the mechanical strength is more pronounced and shows an

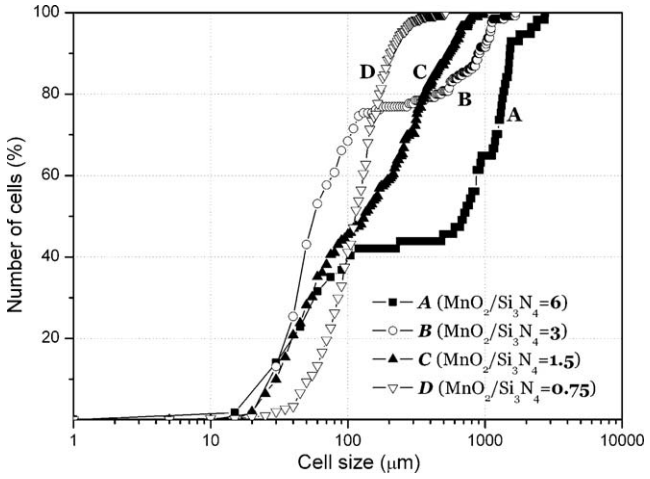

Fig. 3. Cell size distribution of glass foams as a function of MnO_2 amount (Si_3N_4 = 3.5 wt%).

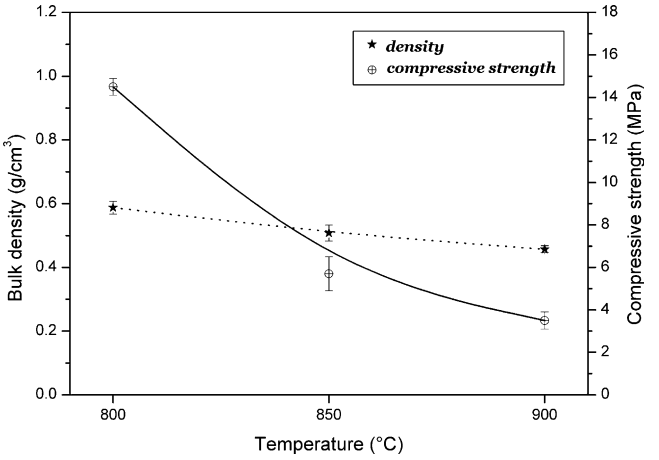

Fig. 4. Evolution of bulk density and compressive strength with firing temperature (Si_3N_4 = 3.5 wt%; MnO_2/Si_3N_4 = 1.5).

exponential trend, which is similar to the one seen for the experiments discussed earlier. Fig. 5 shows that for the lowest temperature (800 °C) the morphology of the porosity consists of small spherical pores (150 μm), in which the ratio between the area occupied by the cells walls and the total area is relatively high. With increasing foaming temperature (850 and 900 °C), the amount of porosity and the cell size increase due to the increased gas pressure and the lowered glass viscosity, with the beginning of some coalescence. At 900 °C, the cell size distribution is again clearly bimodal (see right side of Fig. 5).

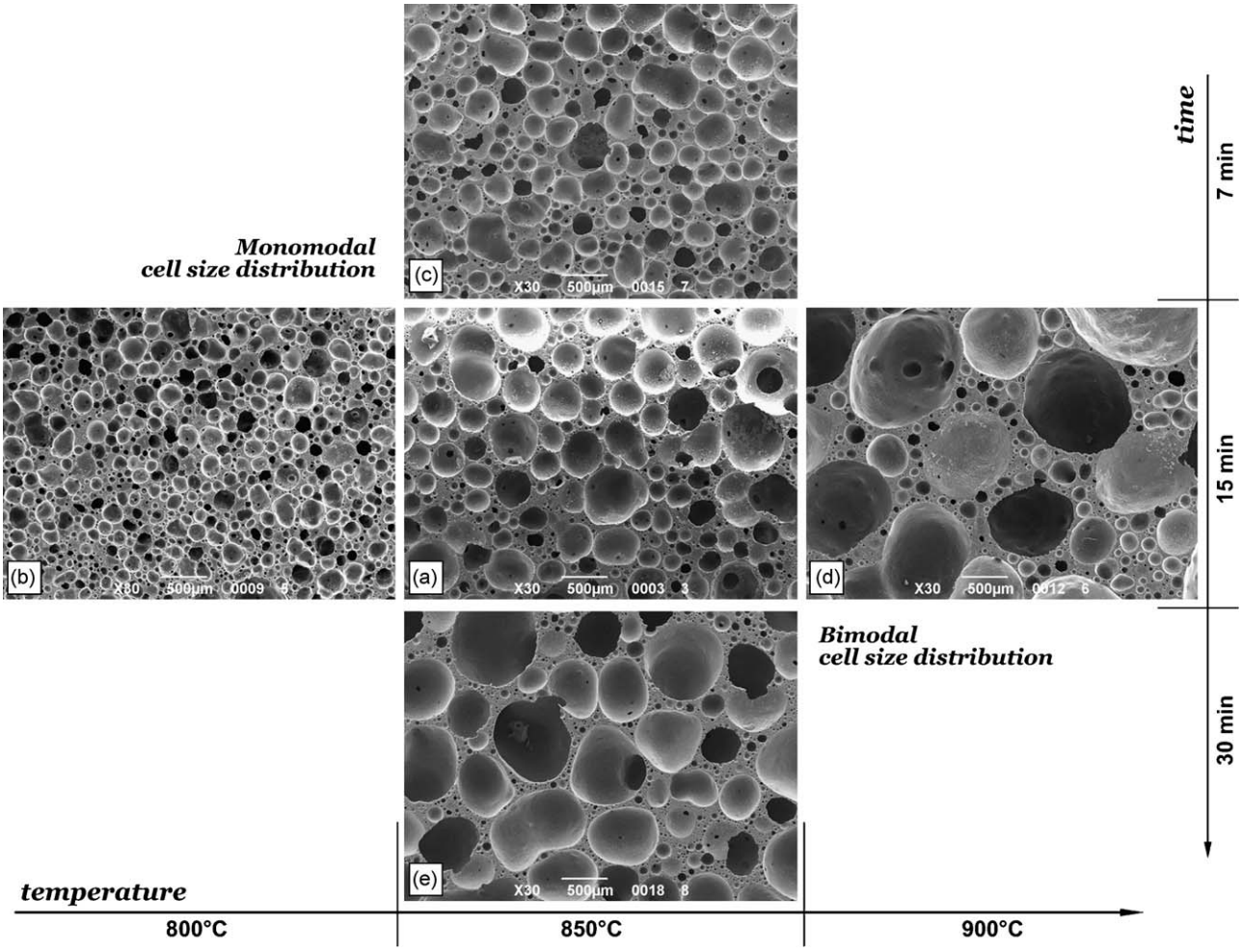

Fig. 5. Microstructural evolution of glass foams with temperature (Si_3N_4 = 3.5 wt%; MnO_2/Si_3N_4 = 1.5) and soaking time: (a) 850 °C, 15 min; (b) 800 °C, 15 min; (c) 850 °C, 7 min; (d) 900 °C, 15 min; (e) 850 °C, 30 min.

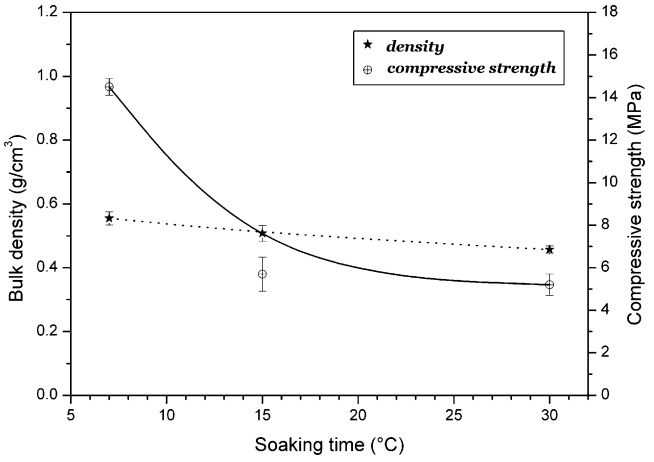

Fig. 6. Evolution of bulk density and compressive strength with soaking time (Si_3N_4 = 3.5 wt%; MnO_2/Si_3N_4 = 1.5; soaking temperature = 850 °C).

When the processing temperature is kept constant at 850 °C (again with MnO_2/Si_3N_4 = 1.5), the soaking time is then another important factor affecting the microstructure of the samples. Fig. 6 shows that the bulk density does not vary significantly with soaking time at 850 °C. On the contrary, compressive strength decreases going from 7 to 15 min of soaking time, and then stabilizes. The SEM micrographs shown in Fig. 5, illustrating the evolution of the microstructure of foamed samples, demonstrate that the cell coalescence may be reduced by limiting the soaking time. Once a certain level of porosity is obtained (by the action of MnO_2 and/or temperature) it is important to stop, by interrupting the fabrication process, the coalescence and the transformation of the cell size distribution from monomodal to bimodal, as they contribute to the decrease in strength of the components.

This concept is summarized in Fig. 7, which reports a "specific compressive strength" parameter, i.e. the ratio between compressive strength and bulk density, for foams with a similar porosity degree, i.e. those obtained with MnO_2/Si_3N_4 = 1.5 at 850 °C, for 7 and 15 min, and at 800 °C, for 15 min. Classical models for compressive strength of foams,

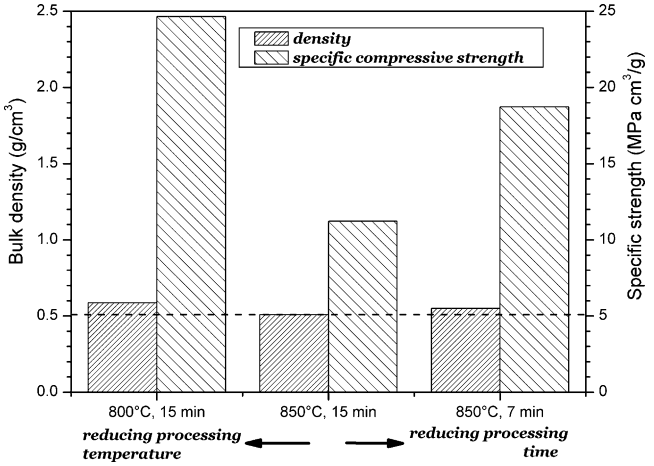

Fig. 7. Effect of the reduction of processing temperature and processing time on the bulk density and specific strength of glass foams.

provided by Gibson and Ashby [23,24], predict the dependence of strength (σ_{cr}) on the flexural strength of the solid phase (σ_{fs}) and, above all, on the relative density (ρ_r), i.e. the ratio between bulk density and true density, as a combination of exponential and linear terms, as follows:

$$\frac{\sigma_{cr}}{\sigma_{fs}} \approx 0.2(\Phi\rho_r)^{3/2} + (1-\Phi)\rho_r \quad (2)$$

The quantity $(1-\Phi)$ expresses the fraction of solid in the cell walls; if the foam is open celled, the pores are fully interconnected, with material only on the cell edges, so that $\Phi = 1$ $(1-\Phi = 0)$ and the exponential term is dominant; on the contrary, for a closed cell foam, Φ is lower, with some material constituting the cell walls, and the strength is mostly given by the linear term. Since the flexural strength and the true density are practically constant (it was observed that different foaming conditions did not cause any crystallization of the glass), the specific compressive strength parameter here introduced could be considered as an index of the sensitivity of the strength with respect to the exponential term. If the strength was only linearly dependent on density, the specific strength should be almost constant for foams with a similar porosity. Fig. 7 highlights, however, a significant difference of specific strength for a limited difference in density. The strength of the foam prepared at 850 °C for 15 min, the one with the minimum specific strength, is fitted by Eq. (2) (with a flexural strength of 70 MPa, a typical value for soda-lime glass [22] and a true density equal to that of the starting glass) by assuming a Φ parameter equal to 0.65. The strength values of the other foams are fitted with a much lower Φ parameter (0.35 for 850 °C, 7 min, and 0.12 for 800 °C, 15 min). The almost monomodal cell size distribution, provided by the reduction of temperature and soaking time, therefore maximizes the strength by making the foams more similar to ideal closed cell foams, i.e. with non-porous cell walls. The reduction of firing time is probably the most useful parameter for mechanical properties optimization, since it leads to an improvement in strength without significantly increasing the density of the foam, and enables very fast processing cycles.

4. Conclusions

We may conclude that

1) MnO_2 effectively promotes the oxidation of Si_3N_4, maximizing its foaming action in softened glass, at a relatively low temperature (much lower than that required for the decomposition of pure silicon nitride);
2) High levels of porosity in glasses foamed with Si_3N_4/MnO_2 are associated with cell coalescence and bimodal cell size distribution, which negatively affect the mechanical properties;
3) The microstructural evolution may be controlled by lowering the processing temperature or reducing the soaking time, both effective in avoiding cell coalescence and promoting a monomodal cell size distribution.

Acknowledgments

This study was funded by the Instituto de la Mediana y Pequeña Empresa Valenciana (IMPIVA) in the framework of the program ''Programa de alta especialización en tecnologías industriales'', and by the Ministerio de Educación y Ciencia in the frame of the program ''Plan Nacional de I+D+i, 2004–2007'', project reference: BIA2006-14242.

References

[1] G. Scarinci, G. Brusatin, E. Bernardo, Production technology of glass foams, in: M. Scheffler, P. Colombo (Eds.), Cellular Ceramics. Structure, Manufacturing, Properties and Applications, Wiley–VCH, Weinheim, Germany, 2005.
[2] G.W. Mc Lellan, E.B. Shand, Glass Engineering Handbook, McGraw-Hill Book Co., New York, 1984 (Chapter 19).
[3] A. Mueller, S.N. Sokolova, V.I. Vereshagin, Characteristics of lightweight aggregates from primary and recycled raw materials, Constr. Build. Mater. 22 (April (4)) (2008) 703–712.
[4] W.O. Lytle (Pittsburgh Plate Glass, USA), US Patent 2,215,223 (1940).
[5] B.K. Demidovich, Production and Application of Glass Foam, Nauka i Tekhnika, Minsk, 1972 (in Russian).
[6] E.H. Haux (Pittsburgh Plate Glass, USA), US Patent 2,191,658 (1940).
[7] W.D. Ford (Pittsburgh Corning, USA), US Patent 2,691,248 (1954).
[8] W. Owen (Pittsburgh Plate Glass, USA), US Patent 2,310,457 (1943).
[9] P. Colombo, G. Brusatin, E. Bernardo, G. Scarinci, Inertization and reuse of waste materials by vitrification and fabrication of glass-based products, Curr. Opin. Solid State Mater. Sci. 7 (2003) 225–239.
[10] E. Bernardo, G. Scarinci, S. Hreglich, Foam glass as a way of recycling glasses from cathode ray tubes, Glass Sci. Technol. 78 (2005) 7–11.
[11] E. Bernardo, F. Albertini, Glass foams from dismantled cathode ray tubes, Ceram. Int. 32 (2006) 603–608.
[12] F. Méar, P. Yot, M. Ribes, Effects of temperature, reaction time and reducing agent content on the synthesis of macroporous foam glasses from waste funnel glasses, Mater. Lett. 60 (2006) 929–934.
[13] F. Méar, P. Yot, R. Viennois, M. Ribes, Mechanical behaviour and thermal and electrical properties of foam glass, Ceram. Int. 33 (2007) 543–550.
[14] E. Bernardo, R. Cedro, M. Florean, S. Hreglich, Reutilization and stabilization of wastes by the production of glass foams, Ceram. Int. 33 (2007) 963–968.
[15] H.R. Fernandes, D.U. Tulyaganov, J.M.F. Ferreira, Preparation and characterization of foams from sheet glass and fly ash using carbonates as foaming agents, Ceram. Int. 35 (2009) 229–235.
[16] E. Bernardo, Micro- and macro-cellular sintered glass–ceramics from wastes, J. Eur. Ceram. Soc. 27 (2007) 2415–2422.
[17] V. Ducman, M. Kovačević, The foaming of waste glass, Key Eng. Mater. 132–136 (1997) 2264–2267.
[18] J.E. Post, Manganese oxide minerals: crystal structures and economic and environmental significance, Proc. Natl. Acad. Sci. U.S.A. 96 (1999) 3447–3454.
[19] K.L. Berg, S.E. Olsen, Kinetics of manganese ore reduction by carbon monoxide, Metall. Mater. Trans. 31B (2000) 477–490.
[20] H. Scholze, Glass. Nature, Structure and Properties, Springer-Verlag, Berlin, 1991.
[21] A. Ray, A.N. Tiwari, Compaction and sintering behaviour of glass–alumina composites, Mater. Chem. Phys. 67 (2001) 220–225.
[22] E. Bernardo, G. Scarinci, A. Maddalena, S. Hreglich, Development and mechanical properties of metal-particulate glass matrix composites from recycled glasses, Composites A 35 (2004) 17–22.
[23] L.J. Gibson, M.F. Ashby, Cellular Solids, Structure and Properties, Cambridge University Press, Cambridge, UK, 1999.
[24] E. Bernardo, P. Colombo, Cellular structures, in: R. Riedel, I.-W. Chen (Eds.), Ceramic Science and Technology, Volume 1, Structures, Wiley–VCH Verlag GmbH, Weinheim, Germany, 2008.
[25] J.S. Morgan, J.L. Wood, R.C. Bradt, Cell size effects on the strength of foamed glass, Mater. Sci. Eng. 47 (1981) 37–42.